

Please cite this article in press as: Carpaneto J, et al., Decoding the activity of grasping neurons recorded from the ventral premotor area F5 of the macaque monkey, *Neuroscience* (2011), doi: 10.1016/j.neuroscience.2011.04.062

Neuroscience xx (2011) xxx

DECODING THE ACTIVITY OF GRASPING NEURONS RECORDED FROM THE VENTRAL PREMOTOR AREA F5 OF THE MACAQUE MONKEY

J. CARPANETO,^a M. A. UMITÀ,^{b,c} L. FOGASSI,^{b,c,d}
A. MURATA,^e V. GALLESE,^{b,c}
S. MICERA^{a,f} AND V. RAOS^{g,h*}

^aThe BioRobotics Institute, Scuola Superiore Sant'Anna, Pisa, Italy

^bDepartment of Neuroscience, Section of Physiology, University of Parma, Parma, Italy

^cItalian Institute of Technology, Brain Center for Social and Motor Cognition, Section of Parma, Parma, Italy

^dDepartment of Psychology, University of Parma, Parma, Italy

^eDepartment of Physiology, Kinki University Faculty of Medicine, Osaka-Sayama, Japan

^fInstitute for Automation, Swiss Federal Institute of Technology, Zurich, Switzerland

^gDepartment of Basic Sciences, Faculty of Medicine, School of Health Sciences, University of Crete, Iraklion, Greece

^hFoundation for Research and Technology-Hellas, Institute of Applied and Computational Mathematics, Iraklion, Greece

Abstract—Many neurons in the monkey ventral premotor area F5 discharge selectively when the monkey grasps an object with a specific grip. Of these, the motor neurons are active only during grasping execution, whereas the visuomotor neurons also respond to object presentation. Here we assessed whether the activity of 90 task-related F5 neurons recorded from two macaque monkeys during the performance of a visually-guided grasping task can be used as input to pattern recognition algorithms aiming to decode different grips. The features exploited for the decoding were the mean firing rate and the mean interspike interval calculated over different time spans of the movement period (all neurons) or of the object presentation period (visuomotor neurons). A support vector machine (SVM) algorithm was applied to the neural activity recorded while the monkey grasped two sets of objects. The *original* set contained three objects that were grasped with different hand shapes, plus three others that were grasped with the same grip, whereas the six objects of the *special* set were grasped with six distinctive hand configurations. The algorithm predicted with accuracy greater than 95% all the distinct grips used to grasp the objects. The classification rate obtained using the first 25% of the movement period was 90%, whereas it was nearly

perfect using the entire period. At least 16 neurons were needed for accurate performance, with a progressive increase in accuracy as more neurons were included. Classification errors revealed by confusion matrices were found to reflect similarities of hand grips used to grasp the objects. The use of visuomotor neurons' responses to object presentation yielded grip classification accuracy similar to that obtained from actual grasping execution. We suggest that F5 grasping-related activity might be used by neural prostheses to tailor hand shape to the specific object to be grasped even before movement onset. © 2011 IBRO. Published by Elsevier Ltd. All rights reserved.

Key words: ventral premotor cortex, decoding, grasping, hand configuration, neuroprosthesis.

The plethora of bones, joints and muscles constituting the hand, gives to this structure remarkable biomechanical complexity. From the kinematic point of view, the hand has over 20 degrees of freedom (DOFs) (Kapandji, 1982; Soechting and Flanders, 1997). The control of multi-DOFs artificial hand prosthesis which is capable of carrying out many dexterous tasks in an effective and flexible way (Light and Chappell, 2000; Carrozza et al., 2006) is particularly challenging. Psychophysical studies suggested that the brain adopts simplifying strategies in order to reduce the complexity of hand movements by controlling the different fingers in a "synergic" way (Santello et al., 1998; Mason et al., 2001; Schieber and Santello, 2004). In the last years many researchers have attempted to use cortical neuronal activity to develop brain-machine interfaces (BMIs) for both reaching and grasping (Wessberg et al., 2000; Serruya et al., 2002; Taylor et al., 2002; Carmena et al., 2003; Musallam et al., 2004; Hochberg et al., 2006; Kim et al., 2006; Santhanam et al., 2006; Velliste et al., 2008; for review, see Schwartz et al., 2006; Hatsopoulos and Donoghue, 2009; Nicolelis and Lebedev, 2009).

There are several cortical areas whose neurons fire when hand movements are executed (Murata et al., 1997, 2000; Raos et al., 2003, 2004, 2006; Brochier and Umiltà, 2007; Gardner et al., 2007a,b; Umiltà et al., 2007; Rozzi et al., 2008; Baumann et al., 2009; Bonini et al., 2010; Fattori et al., 2010) and thus could, in principle, provide reliable and robust signals for the control of skilful grasping by an artificial hand. Among them is the rostral sector of the ventral premotor cortex (area F5, Matelli et al., 1985) which contains neurons that code specific goal-related distal motor acts and not single movements (Rizzolatti et al., 1988; Murata et al., 1997; Raos et al., 2006; Umiltà et al., 2007). F5 grasping neurons usually show specificity for the type of

*Correspondence to: V. Raos, Department of Basic Sciences, Faculty of Medicine, University of Crete, P.O. Box 2208, 710 03 Iraklion, Crete, Greece. Tel: +30-2810-394512; fax: +30-2810-394530.

E-mail address: vraos@med.uoc.gr or vasraos@gmail.com (V. Raos).
Abbreviations: AIP, anterior intraparietal area; ANN, artificial neural network; BMI, brain-machine interface; CM, confusion matrix; DOFs, degrees of freedom; kNN, k-nearest neighbor; LC, linear classifier; LED, light-emitting diode; LOO, leaving-one-out; MD, movement in dark condition; mFR, mean firing rate; MI, primary motor cortex; mISI, mean interspike interval; ML, movement in light condition; OF, object fixation; PI, preference index; PMd, dorsal premotor cortex; RBF, radial basis function; RR, recognition ratio; SM, softmax network; SVM, support vector machines.

0306-4522/11 \$ - see front matter © 2011 IBRO. Published by Elsevier Ltd. All rights reserved.
doi:10.1016/j.neuroscience.2011.04.062

prehension (precision grip, finger and whole hand prehension) performed to grasp an object. As originally proposed by Rizzolatti and colleagues (1988) area F5 contains a “vocabulary” of elementary motor acts in which each “word” corresponds to a category of motor neurons that represent either the goal of the motor act, or the way in which it is executed, or its temporal segmentation. In addition to motor-related discharge, some F5 neurons also respond to the presentation of an object or a set of objects, even when grasping is not actually performed. Often the object evoking the strongest activity during grasping also evokes optimal activity during its visual presentation (Rizzolatti et al., 1988; Murata et al., 1997; Raos et al., 2006). Hierarchical cluster analysis indicated that the selectivity of both the motor and the visual discharge of grasping-related F5 neurons is not determined by the object shape but by the grip posture used to grasp the object (Raos et al., 2006).

The goal of the present study was to explore whether neural activity recorded from area F5 can provide a reliable signal to pattern recognition algorithms in order to decode the hand configuration to be used for grasping an object. We demonstrated that the recognition algorithm, based on the motor and visual discharge of F5 grasping-related neurons, is able to predict with accuracy distinctive hand shapes.

EXPERIMENTAL PROCEDURES

Properties of the neurons analyzed in this paper have been reported in a previous study (Raos et al., 2006). Single unit activity was recorded from area F5 in the posterior bank of the inferior limb of the arcuate sulcus in three hemispheres (contralateral to the moving forelimb) of two awake monkeys (*Macaca nemestrina*). The behavioral apparatus and paradigm are summarized in the next section (for more details see (Raos et al., 2006)). All experimental protocols were approved by the Veterinarian Animal Care and Use Committee of the University of Parma, and complied with the European law on the humane care and use of laboratory animals.

Behavioral task

The behavioral paradigm required the monkeys either to observe only or to observe and then reach for and grasp 3-dimensional objects. The objects were grasped with different types of grips, according to their physical characteristics (Murata et al., 2000; Raos et al., 2006). The monkey was seated on a primate chair with the head fixed, in front of a rotating turntable subdivided into six sectors, each containing a different object. The objects were presented one at a time. A spot of light from a red/green light-emitting diode (LED) that instructed the behavior of the monkey was projected onto the object through a half mirror. Neurons were tested in three experimental conditions. The conditions, run separately one after the other, were the following: (1) Movement in light condition (ML); (2) Movement in dark condition (MD) and (3) Object fixation (OF). The initial LED color (red or green) used in the movement and fixation conditions, respectively, allowed the monkey to discriminate immediately between the movement and the fixation conditions. The temporal sequence of the events during the four conditions is illustrated in Fig. 1. In the movement conditions the monkey initially had to fixate the red LED for a variable period of 1.0–1.2 s. The LED was projected onto the object which was visible only in the ML condition. A change of LED color instructed the monkey to reach for and grasp the object, pull,

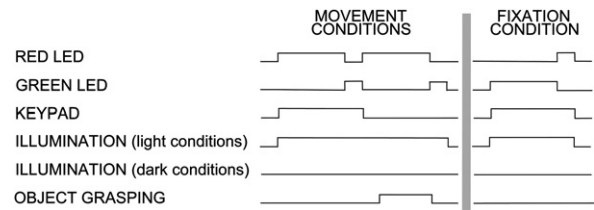


Fig. 1. Timeline of the task events in movement and fixation conditions. Upward deflection: on, downward deflection: off.

and hold it for a variable period of 1.0–1.2 s. The reaching-to-grasp movement was performed with and without visual guidance in the ML and MD conditions, respectively. In the OF condition, the monkey had to fixate the presented object for 1–1.2 s while it was engaged in a motor behavior that was irrelevant to the object (a key press). In the ML and OF conditions the objects were presented in random order, in the MD condition the objects were presented in blocks. The task events LED on (red or green), key-press, LED color change (go signal), key release (movement onset in the movement conditions), object pull (movement end), LED color change, and object release have been acquired as digital markers together with the neuronal activity. These markers were used for the alignment of the neuronal activity across the different trials. A more detailed account on the behavioral paradigm can be found in (Raos et al., 2006).

A variety of objects of different sizes and shapes was used. The two monkeys were trained to always use an identical hand posture for grasping the same object. We used a set of six geometric solids (cube, cone, sphere, cylinder, horizontal plate, and horizontal ring), as originally employed by Sakata and co-workers (Murata et al., 1996, 1997; Raos et al., 2006). This set of objects will be referred to as “original turntable.” The grips with which the objects were grasped are the following. Sphere, cone, and cube: side grip performed using the thumb and the radial surface of the distal phalanx of the index finger. Cylinder: finger prehension performed using the first three fingers. Horizontal plate: primitive precision grip performed using the thumb and the radial surface of the middle and distal phalanges of the index finger. Horizontal ring: hook grip with the fingers inserted into the ring.

To test a broader variety of grips we introduced another set of objects that will be referred to as “special turntable.” This set was composed of the following objects: small sphere, small horizontal ring, large horizontal ring, small sphere in horizontal groove, large cylinder in horizontal container, and very large sphere. The small sphere in horizontal groove was grasped with advanced precision grip performed with the pulpar surface of the last phalanx of the index finger opposed to the pulpar surface of last phalanx of the thumb. For grasping the large cylinder in horizontal container, all the fingers were inserted into the container, with the four fingers opposed to the thumb. The prehension of the very large sphere required all the fingers to wrap around the object and the palm to be in contact with the object. A summary of the objects and the grips is provided in Fig. 1.

Neuronal properties

Single-unit activity was recorded from area F5 in the posterior bank of the inferior limb of the arcuate sulcus in three hemispheres (contralateral to the moving forelimb) of two awake monkeys (*Macaca nemestrina*). Surgical and recording procedures were previously described (Raos et al., 2006). Data from 90 task-related grasping neurons have been analyzed in the present study. Sixty-five neurons were tested with the objects of the original turntable and 25 with the objects of the special turntable. The recorded neurons were subdivided into two main classes: motor

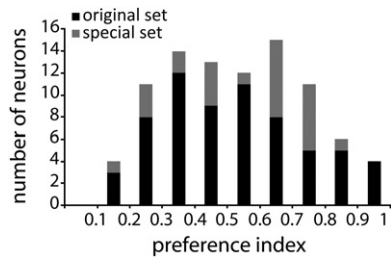


Fig. 2. Distribution of the preference index (PI). Black bars: original set, 65 neurons; grey bars: special set, 25 neurons.

neurons ($n=46$, 36 tested with the original set of objects, 10 tested with the special set of objects) and visuomotor neurons ($n=44$, 29 tested with the original set of objects, 15 tested with the special set of objects). All neurons of both classes discharged during grasping movements. Visuomotor neurons, in addition, also responded during object presentation.

To obtain a measure of the motor preference of the recorded neurons we computed a preference index (PI) that takes into account the magnitude of the neuron response during the grasping of the objects, as follows:

$$PI = (n - (\sum r_i / r_{max})) / (n - 1)$$

where n is the number of objects, r_i the activity for object i , and r_{max} the maximum activity in the movement epoch of the ML condition. The PI can range between 0 and +1.0. A value of 0 indicates the same magnitude of response for all six objects, while a value of 1 indicates preference for only one object. The distribution of the PIs, for the neurons tested with the objects of the original and the special set, calculated from the activity in the movement epoch of the ML condition is presented in Fig. 2.

Hierarchical cluster analysis showed that the determinant of the selectivity of F5 neurons was the grip used to grasp an object and not the shape of the object (Raos et al., 2006). Consequently, the objects of the original set have been grouped as follows: the ring—the only object that does not require the opposition of the thumb to be grasped—is separated from all the other objects. Out of the remaining five objects, for which the use of the thumb is necessary, the elongated objects (plate and cylinder) which are grasped with a similar type of grip are at a close distance; the cube, the sphere, and the cone which are grasped in an identical

way (side grip) form a single cluster. For the objects of the special set, the two rings, which do not require the opposition of the thumb, form a cluster separated from the other objects. The grasping of the remaining four objects requires the involvement of the thumb. This digit acts as a buttressing and reinforcing agent for the grasping of the very large sphere. Therefore, this object is separated from the small sphere, the sphere in groove, and the cylinder in container which require an active opposition of the thumb to the other fingers and are clustered together. Fig. 3 provides a summary of the clustering among grips in both sets of objects used.

Selection of neuronal features and time periods for analysis

The features selected for the decoding were the mean firing rate (mFR) and the mean interspike interval (mISI). The combined use of these two features outperformed the use of each one in isolation (data not presented in the manuscript). The distributions of the frequency rates and interspike intervals within the trials during the whole movement period (entire neuronal population) are presented in Fig. 4A, B.

Different amount of time was required for grasping the various objects with the appropriate grips (Table 1). The features during the movement period (from the onset of reaching movement to the beginning of object pulling), in the ML and MD conditions of all the neurons, were calculated over four time-spans corresponding to 25%, 50%, 75%, and 100% of movement time. To avoid incorrect classification of the grips due to the variation of the movement time periods among grips and trials, mFR and mISI were estimated on a trial-by-trial basis, namely four different values per trial were taken (first quarter, half, three quarters and whole movement interval).

For a given condition (e.g. ML), for a given time span (e.g. 75% of movement time), for a given number of neurons (e.g., K), and for a given object to be grasped, the structure of the feature vector was the following:

```
FR_neuron_1 ISI_neuron_1 ... .. FR_neuron_K ISI_neuron_K
```

Given that the visuomotor neurons respond to the presentation of an object or a set of objects, even when a grasping movement is not required, we also analyzed four time-spans (25%, 50%, 75%, and 100%) of the object presentation period, 1–1.2 s, from the illumination of the object to the cue signaling the

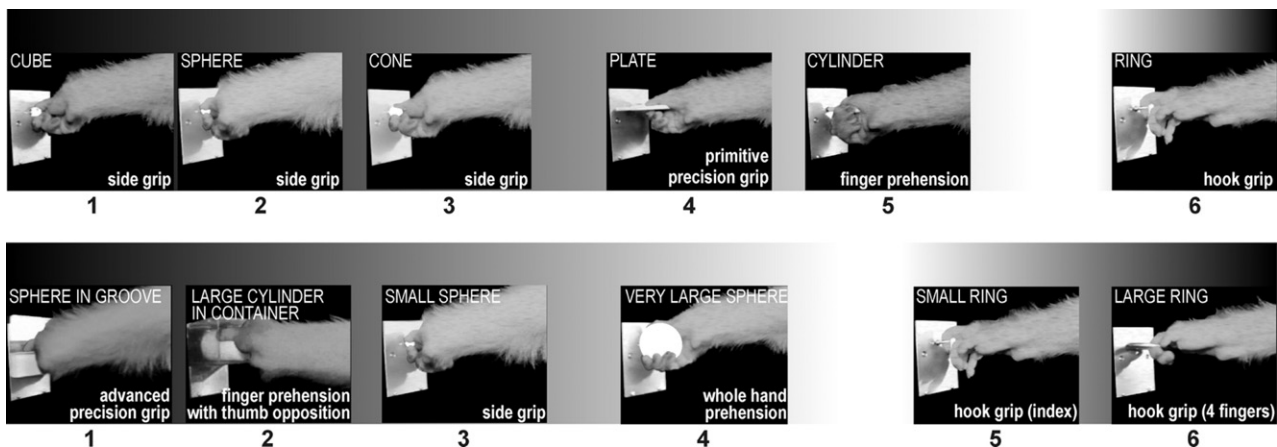


Fig. 3. Video frames illustrating the grips used by the monkeys for grasping the objects of the original (top) and the special (bottom) set. The numbers 1–6 below each picture denote the code used in the following figures. The distance between the frames as well as the shading of the background denote the similarities among the grips as revealed by hierarchical cluster analysis. The more similar the grips, smaller the distance among the frames and darker the background.

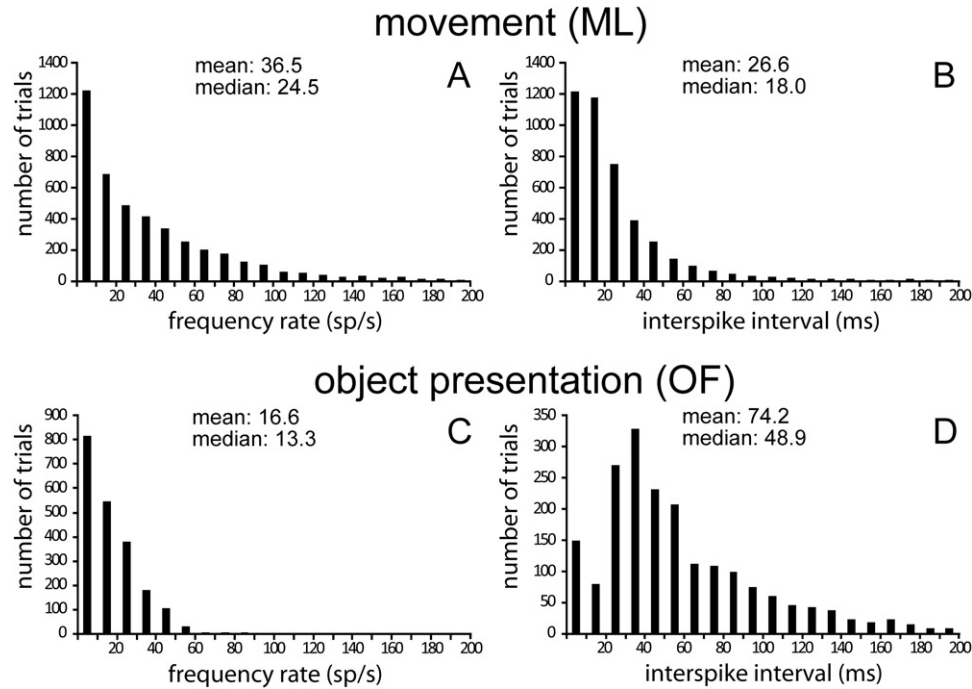


Fig. 4. Distributions of the frequency rates and interspike intervals during (A, B) the entire movement period of ML condition (all neurons, $n=90$) and (C, D) the object presentation period of OF condition (all visuomotor neurons, $n=44$).

release of the key, in the ML and OF conditions of the visuomotor neurons. The distributions of the frequency rates and interspike intervals within the trials during the object presentation period of OF condition (all visuomotor neurons) are presented in Fig. 4C, D. The discharge of the visuomotor units during the object presentation period has been also analyzed, on non-normalized data, in eight time increments with a step of 100 ms, starting 150 ms after the presentation of the object. Hence, the increments used were: 150–250 ms, 150–350 ms . . . 150–950 ms. The first 150 ms of the object presentation period have been omitted to take into account the delay of the visual response with respect to object presentation.

To investigate when, in real time, a reliable grip classification is obtained, features have been extracted from motor and visuomotor units during the period starting 400 ms before the instruction to move (LED color change) and ending 200 ms after the movement onset (key release). In particular, two different approaches were used. In the first one, the features were extracted from a time window of 200 ms which progressively slid over the reference period with a moving step of 50 ms, while in the second, the features were extracted from a time window (initial width: 20 ms) which was progressively increasing at 20 ms increments until to cover the entire reference period.

Table 1. Duration of the movement period (tmov) for the grips tested, calculated as the difference between object pull and key release events of the task

Original set	tmov (ms)	Special set	tmov (ms)
Cube	367±117	Sphere in groove	678±161
Sphere	323±64	Large cylinder in container	518±145
Cone	379±126	Small sphere	415±96
Plate	283±49	Very large sphere	239±38
Cylinder	289±137	Small ring	437±128
Ring	378±108	Large ring	212±50

Decoding algorithms

The performance of several classifiers frequently used in pattern recognition problems such as normal densities based linear classifier (LC) (Fukunaga, 1990), k-nearest neighbor (kNN) (Fukunaga, 1990), artificial neural network (ANN) (Bishop, 1995), softmax network (SM) (Bishop, 1995), and support vector machines (SVM) (Cortes and Vapnik, 1995) have been tested using the F5 data. Their main characteristics are described hereafter.

LCs are the simplest and perhaps the most widely used classifiers. They are based on the normal distribution:

$$p(x|\omega_i) = \frac{1}{(2\pi)^{\frac{1}{2}}|\Sigma_i|^{\frac{1}{2}}} \exp\left\{-\frac{1}{2}(x - \mu_i)^T \Sigma_i^{-1}(x - \mu_i)\right\}$$

A pattern x is assigned to the category ω_i for which the posterior probability, $p(\omega_i|x)$, is the greatest, or equivalently $\log(p(\omega_i|x))$. The means (μ_i) and the covariance matrices (Σ_i) of the categories are estimated from the training data. Data samples often are not normally distributed and for this reason the final error could differ from the optimal Bayesian error.

The kNN classifier is another method based on a measure of the similarity between a new pattern and a set of prototypes for each category in the training set. kNN algorithm finds, for a given input feature x , the k "closest" examples in the training data set and assign x to the category that appears most frequently within the k -subset. This algorithm has been shown to be a robust classifier, especially when the number of training samples is not large as in our case.

ANNs are algorithms originally inspired by the functioning of biological neurons. The basic components of ANN are neurons and connections among them. In a feed-forward neural network structure, a unit receives information from several units belonging to the previous layer. Several ANN structures have been developed in the past (Bishop, 1995): the most popular model is the multi-layer perceptron that consists of an input layer, many intermediate (hidden) layers, and an output layer with an adjustment of

the parameters (weights) based on error back-propagation. Thanks to the non linear relationship between inputs and outputs, ANN are powerful classifiers and are widely used in the field of machine learning even if they have a high computational cost and uncertainty about the working procedure of the classifier. In the present study a feed-forward ANN classifier with 10 hidden units trained using the back-propagation algorithm has been used. The training phase was either stopped after a specified number of epochs (1000), or if the iteration number exceeded twice that of the best classification result.

SVMs are a family of supervised learning methods originally proposed for two-category discrimination problems. Feature vectors are non-linearly mapped to a very high-dimension space where a linear separation between the two categories may be possible. In the transformed feature space a hyperplane is constructed to maximize the margin between category members. Kernel functions are used to avoid the computational costs of the explicit representation of the input vectors in the high dimensional feature space. Moreover, other properties of SVM are the absence of local minima and the automatic derivation of a network structure that guarantees an upper bound on the generalization error (Burges, 1998; Shawe-Taylor and Cristianini, 2004).

If SVM cannot find a separating hyperplane, a regularization parameter C is introduced to allow misclassification in the training set (Cortes and Vapnik, 1995). The type of SVM used in this manuscript is called ν -SVM (Chen et al., 2005). Among the various kernels available, the radial basis function (RBF) was chosen because it allows fairly complex separation surfaces requiring a reduced number of hyper-parameters to tune (Hsu et al., 2003). The radial basis kernels are of Gaussian form:

$$K(x, y) = \exp(-\gamma(x - y)^2)$$

with x, y as input vectors. It was decided to use fixed hyperparameters, even if this could lead to more conservative results, because tuning them by means of iterative methods requires an additional cross-validation scheme that reduces the already small number of examples available to train and test the classifier. Using ν -SVM with RBF, hyperparameters ν and γ need to be chosen. The regularization parameter ν is an upper bound on the fraction of margin errors and a lower bound on the fraction of support vectors. $\nu=0.5$ was selected because it was considered a good trade-off between allowing training errors and favoring smooth separation surfaces. The parameter γ determines the radius of the RBF. We set $\gamma=1/\rho^2$ where ρ is the radius of the smallest sphere in the input space that contains all feature vectors F of the training set. Keerthi (2002) has shown that it is a good starting point for iterative methods. To allow SVMs, and other binary classifiers, to handle multi-category problems, the latter must be decomposed into several binary problems. Several approaches are possible (Huang et al., 2006), and the most commonly used are: (i) one-against-one and (ii) one-against-the-rest. In this work a one-against-one approach was used where, for a k -category classification problem, $k(k-1)/2$ machines were trained. Each SVM separates a pair of categories and, in the prediction stage, a voting strategy was used where the outcome was the category with the maximum number of votes.

The SM estimator (Bishop, 1995) is equivalent to a non linear two layer neural network but the output layer was organized into M outputs corresponding to the number of categories to identify. These output units were trained to encode the probabilities of a specific category. Because these outputs are mutually exclusive (i.e., only a specific category is possible), the probabilities were constrained to sum to unity through SM normalization. The activity of output unit i on trial k , y_i^k , was determined according to:

$$y_i^k = \frac{\exp \left\{ \sum_{j=1}^N w_{ij} r_j^k \right\}}{\sum_{i=1}^6 \exp \left\{ \sum_{j=1}^N w_{ij} r_j^k \right\}}$$

where $\{w_{ij}\}_{i=1, \dots, 6; j=1, \dots, N}$ are the weights and $\{r_j^k\}_{j=1, \dots, N}$ are the activities of the F5 neurons on trial k .

Training and cross-validation

Usually, cross-validation consists of splitting the dataset of examples into two (or more) subsets such that supervised training is initially performed on one subset (the training set), while another is retained "blind" (the test set) for later use in validating the trained classifier and assessing its generalization abilities. To deal with the small number of trials available (6 objects \times 8 repetitions), a leaving-one-out (LOO) validation scheme has been implemented (Fukunaga, 1990). LOO uses a single example per category (grip type) as the test set, and the remaining ones as the training set. The error rate is the number of errors on the single test cases divided by the number of repetitions.

Presentation of results

Classification performance has been assessed and presented by using the recognition ratio (RR) and confusion matrixes (CMs). The RR, the overall percentage of correct classification, is the ratio between the number of grips correctly identified and the total number of grips classified. This parameter provides a synthetic indication of the average performance of the system. The confusion matrix CM describes the pattern of errors made by the classifier. Each row indicates the grip, and each column indicates the classifier predictions (as a percentage of trials). Each element CM_{ij} is the number of grips of actual category i , identified (correctly if $i=j$, wrongly if $i \neq j$) as belonging to the predicted category j . The advantage of a confusion matrix is that it facilitates the identification of subsets of categories that the system recurrently confuses.

The algorithm has been tested varying the number of neurons being decoded to determine the effects on the recognition ratio and on the minimum number of neurons needed for a good classification. The number of units K decoded was set from 2 to the maximum number of units recorded for each set of objects and experimental condition. If the number of combinations of neurons taken K at a time was too high, a random selection of 2000 different combinations has been used for the generation of the population patterns of activity. The RR of the classifiers has been also evaluated varying the number of grips, either considering them different for each object (six/set) or taking into account their similarities as revealed by the hierarchical cluster analysis.

All algorithms have been developed under Matlab (Mathworks, Natick MA, USA) environment. The toolbox provided by (Duin et al., 2004) was used for the LC, kNN and ANN classifiers, whereas the toolbox supplied by Sigurdsson (2002) was employed for the SM classifier. The open source library LIBSVM (Chang and Lin, 2001; Hsu et al., 2003) was used for the SVM classifier.

RESULTS

Different algorithms have been tested for the classification of the features extracted from the signals recorded from F5 grasping-related neurons at time intervals spanning from 25% to 100% of movement or object presentation periods, using different sets of objects/grips (original and special, see Fig. 3). In particular, five classifiers have been tested

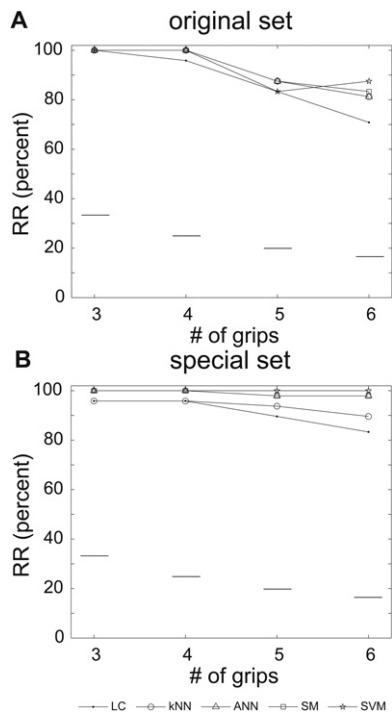


Fig. 5. Comparison of the RR obtained with the different classifiers as a function of the number of grips to be recognized. The entire movement period of ML condition and the entire neuronal population were used for the calculation of RRs. (A) original set; 65 neurons, (B) special set; 25 neurons. Horizontal grey lines denote chance levels.

to discriminate either six grips as if each object required a different grip, or clusters of grips (from three to five) according to the results of the hierarchical cluster analysis. Fig. 5 shows a comparison of the performance of all the classifiers used in this study taking into account the features extracted from the neuronal discharge during the entire movement epoch of the ML condition. Similar results have been obtained with the features extracted from the discharge during the entire movement epoch of the MD condition, as well as during the presentation periods of the ML and OF conditions. For the subsequent analyses we chose to use SVM algorithm because of its higher RR percentage with six grips in both sets of objects (see Fig. 5) and its easier implementation with the data.

Fig. 6 presents the classification performance (RR) as a function of the number of grips to be recognized. We analyzed the neuronal discharge during the movement period of ML and MD condition. When the grips used for grasping the six objects of the original set are considered all different, the performance of the classifier is poor even using the entire movement period (Fig. 6A, C). However, when the classification is made among the four grips actually used in order to grasp the six different objects, the algorithm discriminates accurately (100%) when fractions of the movement time (ML: 50%, MD: 75%) are taken into account (Fig. 6A, C). The performance of the classifier with the six grips of the special set, which appear more distinct than the grips of the original set, reached high values (ML: 100%, MD: 97.92%) when 50% of the movement time is

taken into account (Fig. 6B, D). Note that in the special set of objects there are two objects with the same shape (ring and sphere) but of different size (small and large), which were grasped by the monkey with different grips (see Fig. 3). The algorithm is able to distinguish the objects of different sizes, very likely because its recognition is based on grip coding.

As demonstrated above, a period corresponding to the 50% of the movement time is sufficient for the extraction of the features to obtain correct classification of the grips by the classifier. Given that the time required for the accomplishment of the transport and grasping phases of the movement (calculated as the difference between object pull and key release events) toward the objects of the original and the special set is 337 ± 115 ms and 417 ± 196 ms, respectively, there is sufficient time for the eventual control of a robotic hand. The optimal window length could be selected for each subject as a trade-off between performance and acceptable delay.

In order to investigate the performance of the classifier during the different phases of grasping, we also analyzed the data of the holding phase during which the grips are static. When the grips used for grasping the six objects of the original set are considered all different, the performance of the classifier is poor (Fig. 6E). The performance improves when the classification is made among four grips (91%, with the entire movement period considered). High performance (above 93%) is achieved at short time windows (25%) for the classification of the six grips of the special set (Fig. 6F).

To take advantage of the fact that visuomotor neurons responded also during the presentation of an object or a set of objects, as if the visual features of an object were automatically “translated” into a potential motor act describing its pragmatic physical properties, we also analyzed the neuronal discharge of the object presentation period. Object presentation periods exist in ML and OF conditions. In the former condition, the object presentation period is followed by a grasping movement whereas in the latter it is not. Because both conditions gave equivalent decoding performances, only the results of the OF condition will be presented here. The classifier discriminates accurately (100%) the four grips of the original set when the 25% of object presentation period is used (Fig. 6G). The performance of the classifier for the grips of the special set, although lower than in the latter case, ranges from 91.67% to 95.83% (Fig. 6H).

Fig. 7 presents the classification performance as a function of the number of units recruited for the recognition among the grips. Taking into account the neuronal discharge during the movement period and considering six grips for the objects of the original set, the higher RR (ML: 87.5%, MD: 83.6%) is achieved when the entire movement period and the entire neuronal population is engaged (Fig. 7A, B). However, when the classification is made among four grips, higher RRs (ML: 93.75%, MD: 95.8%) are achieved with 65 neurons recruited, even when only 25% of movement time is used (Fig. 7C, D). The classification performance reaches high values (ML: 94.64–99.87%,

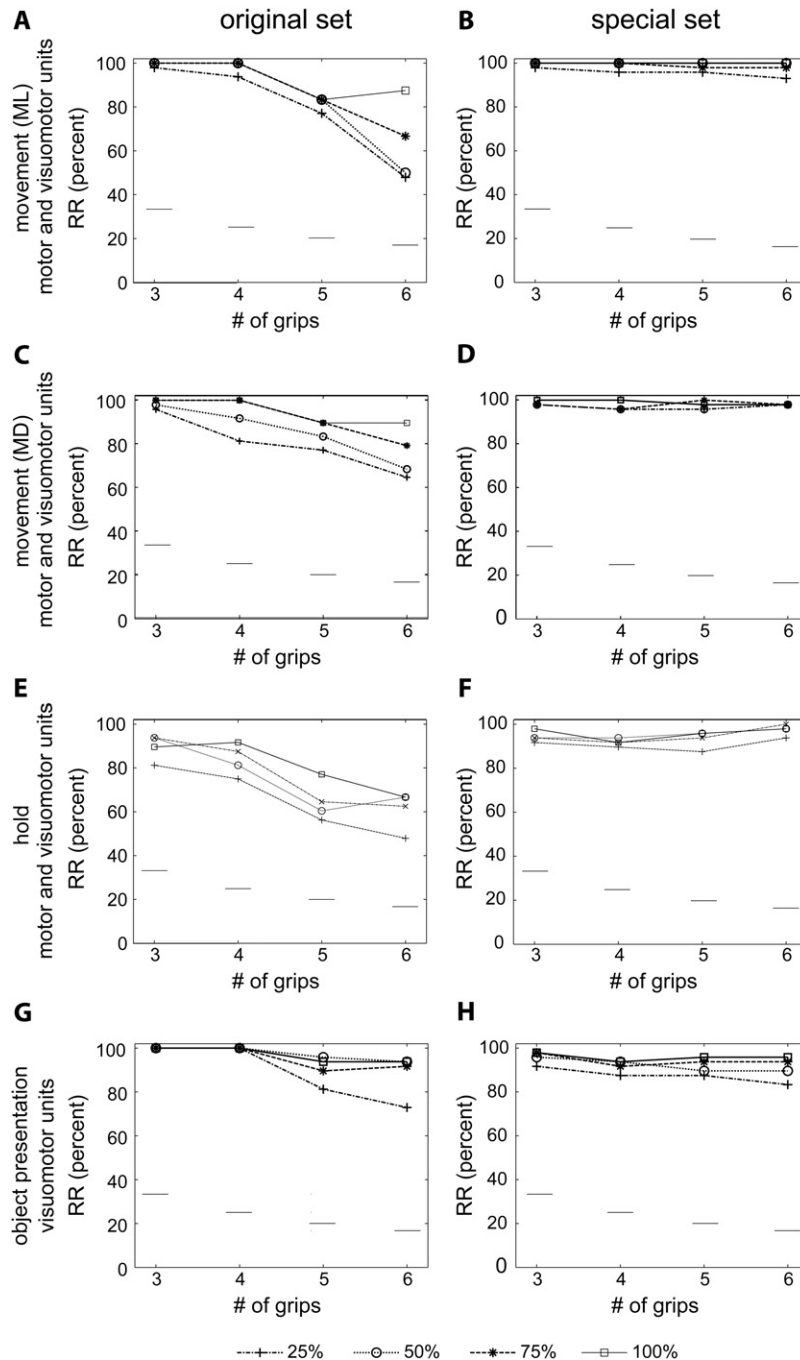


Fig. 6. Performance of the SVM classifier as a function of the number of grips to be recognized based on the features extracted during the 25%, 50%, 75%, and 100% of the movement time of ML (A, B) and MD (C, D) conditions, during the 25%, 50%, 75%, and 100% of the holding period of ML condition (E, F) [all neurons, $n=65$ for the original set (A, C, E) and $n=25$ for the special set (B, D, F)]; as well as during the object presentation period of OF condition [visuomotor neurons, $n=29$ for the original set (G) and $n=15$ for the special set (H)]. Other conventions as in Fig. 5.

MD: 94.64–99.55%) when fewer neurons (16–32) are recruited at longer movement time intervals (50–100%). Concerning the grips for the special set of objects, the accuracy of the recognition reaches high values (ML: 100%, MD: 97.92%) even when few cells (25) were used with a rather short (50%) time window (Fig. 7E, F).

To examine whether and how decoding performance depends on the selectivity of neurons recruited, the popu-

lation of neurons tested with the original set of objects has been divided in two subpopulations on the basis of their motor preference as quantified by the preference index. The neurons having a PI smaller than the median have been assigned to the subpopulation of neurons displaying low selectivity, whereas the neurons having a PI larger than the median constituted the subpopulation of neurons with high selectivity. The performance of the classifier

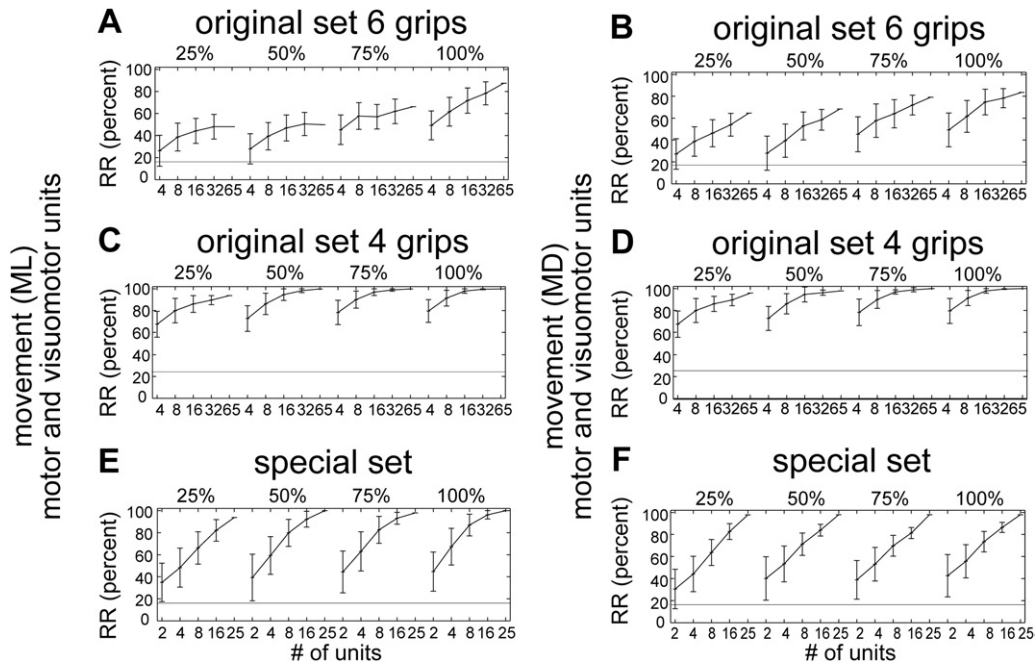


Fig. 7. Performance of the SVM classifier (mean $RR \pm SD$) as a function of the number of neurons based on the features extracted during the 25%, 50%, 75%, and 100% of the movement time of ML (left column) and MD (right column) conditions. (A, B) original set of objects, 65 neurons, six grips; (C, D) original set of objects, 65 neurons, four grips; (E, F) special set of objects, 25 neurons, six grips. Other conventions as in Fig. 5.

using the features extracted during the movement period of the ML condition is presented in Fig. 8. When considering six grips the RR achieved is poor irrespective of low or high selectivity (Fig. 8A, B). However, when the classification is made among four grips, maximum performance is achieved when the entire movement period and all neurons in each subpopulation are taken into account (Fig. 8C, D). It is noteworthy that the classification performance reaches high values (low: 91.95–97.34%, high: 95.52–

96.58%) also when fewer neurons (16–24) are recruited at shorter movement time intervals (50–75%).

Half of the object presentation period and the entire population of the visuomotor neurons tested with the original set are required in order to achieve a high recognition ratio (93.75%) among six grips (Fig. 9A). However, when the classification is made among four grips, the recognition ratio reaches the maximum (100%) using the shortest time window with the entire population (Fig. 9B). Interestingly,

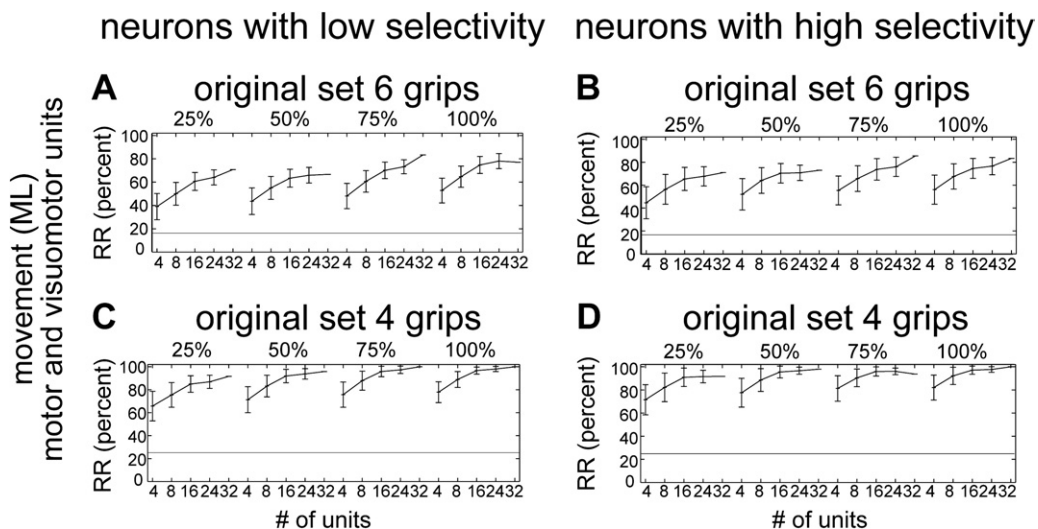


Fig. 8. Performance of the SVM classifier with neurons displaying low (left column) and high (right column) selectivity as quantified by the PI. The SVM classifier (mean $RR \pm SD$) (original set of objects) has been tested as a function of the number of neurons, based on the features extracted during the 25%, 50%, 75%, and 100% of the movement time of ML condition. (A, B) 32 neurons, six grips; (C, D) 32 neurons, four grips. Other conventions as in Fig. 5.

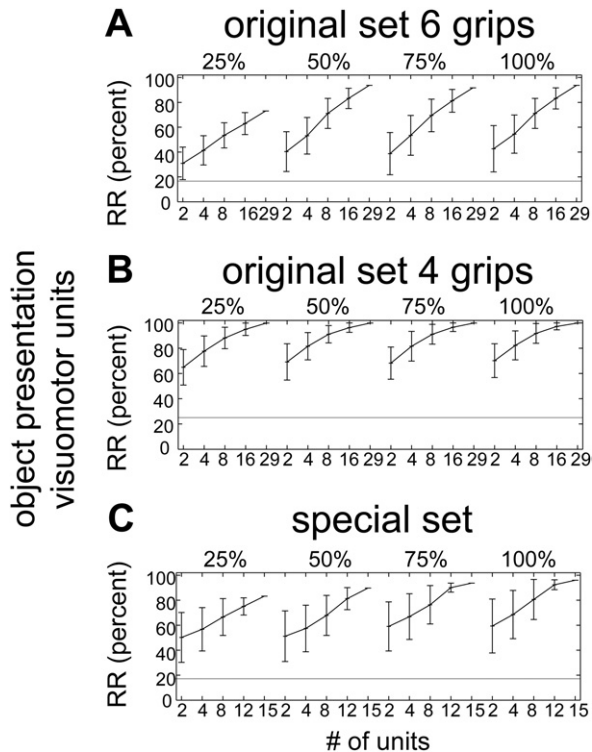


Fig. 9. Performance of the SVM classifier (mean RR \pm SD) as a function of the number of neurons based on the features extracted during the 25%, 50%, 75%, and 100% of the object presentation period of OF condition. (A, B) original set of objects, 29 visuomotor neurons, six and four grips, respectively; (C) special set of objects, 15 visuomotor neurons, six grips. Other conventions as in Fig. 5.

high performance (above 95%) is achieved using fewer units (16) at all time windows (Fig. 9B). The performance of the classifier for the grips of the special set is shown in Fig. 9C. In this case, the entire presentation period is required to achieve the highest recognition (95.83%) among the six grips.

To reveal the effects of the clustering, the CMs presented in Fig. 10 were calculated. In Fig. 10A, C it is evident that the side grips performed for grasping the cube (1), the sphere (2) and the cone (3) cannot be discriminated perfectly even when the entire movement period is used, may be due to the fact that they are virtually identical from a kinematic viewpoint. The grips of the special set are recognized when short fractions of the movement time are employed (Fig. 10B, D), probably due to the sharper kinematic differences among them, as compared to the grips of the original set.

Also in the case of the object presentation period of OF condition the algorithm cannot discriminate satisfactorily among the side grips even when the entire object presentation period is used (Fig. 10E). However, the discrimination among the four grips is achieved with short fractions of the object presentation period (Fig. 10E). The grips of the special set can be recognized without clear effects of clustering when sufficient time is provided (Fig. 10F).

Fig. 11 displays the performance of the SVM as a function of the window length of the object presentation

period of OF condition used for the extraction of the features. For the original set, a period of 450 ms is sufficient to obtain a good prediction of the grips (RRs from 85.42% for six grips to 93.75% for four grips, Fig. 11A). Similarly, a period longer than 650 ms is required to obtain high recognition ratios for the classification of four to six grips during the observation of the objects belonging to the special set (RRs from 93.75% for six grips to 97.92% for four grips, Fig. 11B). Although during object presentation, as compared with movement time, information must be accumulated over longer periods in order for classification to asymptote, the potential use of the discharge during object presentation for the decoding is remarkable given that it occurs well before the initiation of the movement, thus providing ample time for the control of hand prosthesis.

For the results reported so far, the features were calculated on a trial-by-trial basis separately for each portion of the movement period considered, in order to avoid incorrect classification of the grips due to variation of the movement duration among trials and grips. However, this procedure has the disadvantage of missing real time information. To complement our results by defining when one can trust the grip classification in real time, we estimated the performance of the SVM classifier as a function of the number of grips to be recognized based on the features extracted from time spans falling in a reference period starting 400 ms before the instruction to move (LED color change) and ending 200 ms after the movement onset. Fig. 12A, B, E, F show the classification performance when the features were extracted from a time window of 200 ms, which progressively slid over the reference period with a moving step of 50 ms. Fig. 12C, D, G, H show the classification results when the features were extracted from a time window (initial width: 20 ms), which was progressively increasing at 20 ms increments until the end of the reference period. Both approaches revealed that good recognition ratios between the grips can be obtained as early as 400 ms before the instruction to move and that there is no strong difference in the performance of the algorithm before and after movement onset.

DISCUSSION

The results of the present study show that F5 grasping-related neurons represent a reliable source of information for the implementation of decoding algorithms that could eventually be used for the control of artificial hand grasping. In most cases, few neurons and short window lengths for the extraction of the features were sufficient to achieve a good prediction. The classifier could predict the six grips for the special set of objects and the four grips for the original set of objects. Classification errors revealed by confusion matrices were found to reflect similarities of hand postures used to grasp the objects. The decoding process can extract the correct kind of grip even when only the discharge of the visuomotor units during the presentation of the objects (occurring well before movement onset) was used.

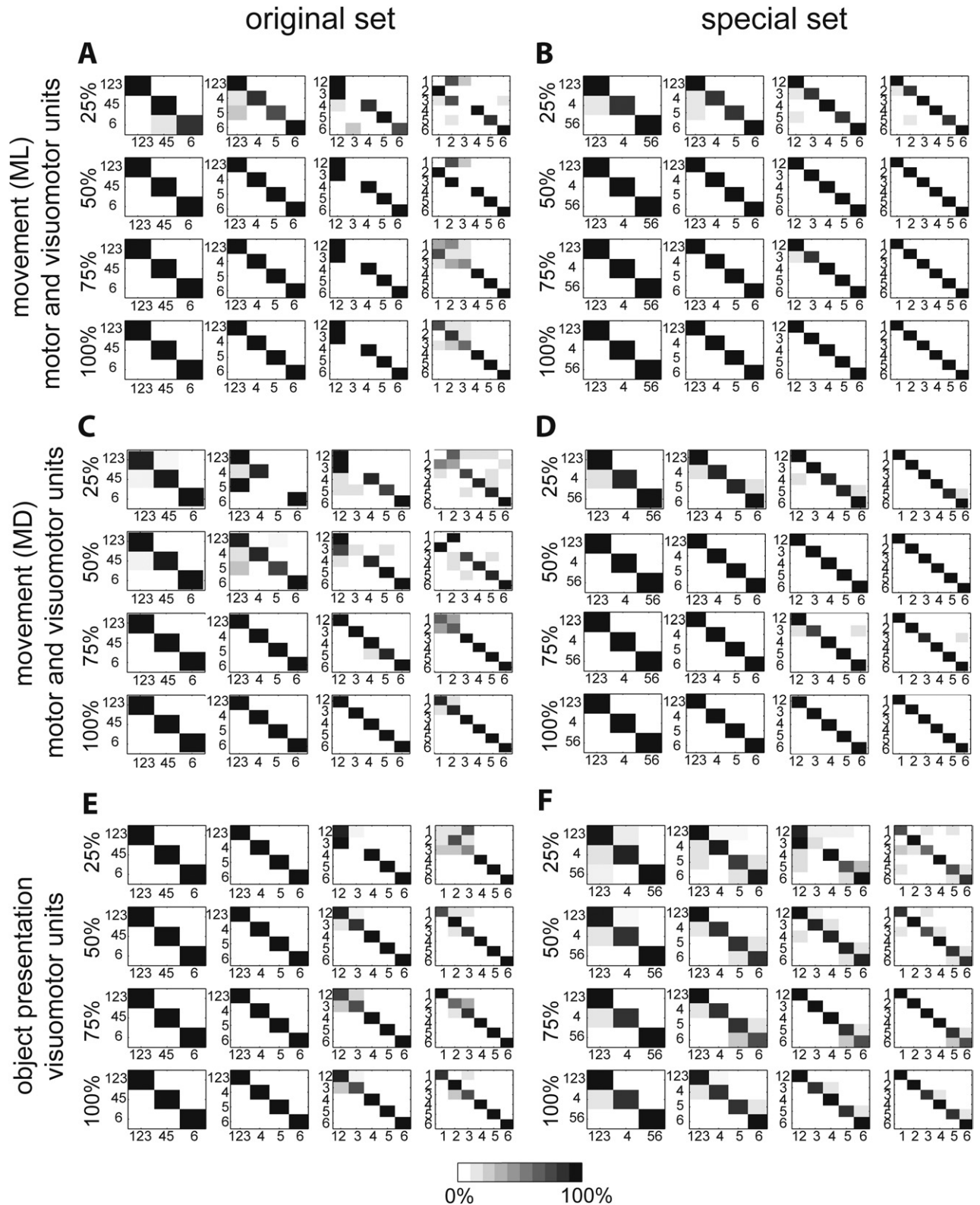


Fig. 10. Confusion matrices (CMs) describing the pattern of errors made by the SVM classifier. Different percentages (25%, 50%, 75%, and 100%) of the movement time of ML (A, B) and MD (C, D) conditions as well as of the object presentation period (E, F) of OF condition have been used for the extraction of the features. Numbers 1 to 6 denote different grips (as presented in Fig. 3) and numbers 12, 123 and 45 denote grips clustered together. The performance of the classifier is represented by the gray shading. (A, C) original set, 65 neurons; (B, D) special set, 25 neurons; (E) original set, 29 visuomotor neurons; (F) special set, 15 visuomotor neurons.

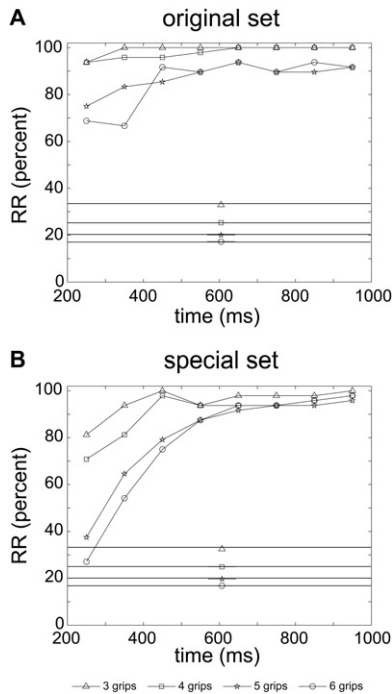


Fig. 11. Comparison of the RRs obtained as a function of the duration of the object presentation period considered. The duration ranges from 150 to 950 ms (steps of 100 ms). (A) original set, 29 visuomotor neurons, (B) special set, 15 visuomotor neurons. Other conventions as in Fig. 5.

The fact that in the present study the decoding was performed offline introduces some caveats. The most important one is related to the use of single cell recordings which provide signals of higher quality (in terms of signal-to-noise ratio) as compared to multiunit activity recorded by chronic implants. We found that the type of grip can be decoded with high accuracy from small numbers of neurons and decoding accuracy remains rather unaffected by the degree of selectivity of the neuronal population. These results likely overstate true performance, as those neurons were selected online for their responsiveness and quality of isolation, something that would not be possible for any currently available implantable system. Therefore, more cells may be necessary to achieve comparable levels of classification performance with chronically implanted electrodes. In addition, our data lack a correlation structure; in contrast, the activities of simultaneously recorded neurons are often correlated. However, it is difficult to predict how the performance would be using the activity of simultaneously recorded neurons because correlations can either improve or deteriorate decoding accuracy depending on the form of the correlation matrix (Zohary et al., 1994; Abbott and Dayan, 1999; Maynard et al., 1999; Bair et al., 2001).

The fact that the decoding performance occurs even when the monkey does not perform the encoded behavior could indicate that the motor timing (movement onset) is not encoded by F5 activity. Recent studies demonstrate that predictions of motor timing can be extracted from the

population activity of neurons recorded in motor and dorsal premotor cortex (Lebedev et al., 2008).

The majority of the studies aimed to decode grasping movements used signals recorded from area MI (Carmena et al., 2003; Hochberg et al., 2006; Kim et al., 2006; Velliste et al., 2008). However, simultaneous recordings from ventral premotor and MI populations revealed that premotor neurons display greater grip specificity than those of MI. The grip-related activity of F5 premotor neurons started in the pre-movement and early movement phases and was a strong predictor of the activity later in the task. In contrast, MI neurons were involved in all phases of the grasp-and-hold task, but their contribution varied during different phases of the tasks (Umiltà et al., 2007). Moreover, it has been shown that F5 neurons are more related to the goal of the motor act than MI neurons do (Umiltà et al., 2008). The ventral premotor area F5 could influence hand motor function through at least two pathways: corticospinal projections (Dum and Strick, 1991; He et al., 1993; Borra et al., 2010) and corticocortical projections to MI (Matsumura and Kubota, 1979; Muakassa and Strick, 1979; Matelli et al., 1986; Dum and Strick, 2005). Several lines of evidence support the notion that the hand motor function is accomplished by the latter pathway (Cerri et al., 2003; Shimazu et al., 2004). Very recently it has been demonstrated that inactivation of MI reduced or abolished electromyographic responses elicited by intracortical microstimulation of F5 (Schmidlin et al., 2008). These results further corroborate the idea that the motor effects evoked from F5 depend, at least in part, on corticocortical interactions with MI, leading to activation of MI corticospinal outputs to hand muscles.

The robotic limbs used in many studies during the last decade were equipped with grippers that could open and close, but lacked the flexibility and adaptability of the human or primate hand and therefore could not change their configuration to conform appropriately to objects that differ in size and shape (Carmena et al., 2003; Hochberg et al., 2006; Kim et al., 2006; Velliste et al., 2008). A BMI aiming to control complex motor actions such as reaching to and grasping objects of different shape and size could take advantage of multiple cortical areas with complementary activities. The use of activities from multiple neuronal populations belonging to different cortical areas would improve decoding performance (Lebedev et al., 2008) and enable the extraction of different kinds of information (Hatsopoulos et al., 2004; Schwartz et al., 2004). Based on simultaneous recordings from MI and dorsal premotor (PMd) cortices in behaving monkeys, Hatsopoulos et al. (2004) demonstrated a double dissociation in which ensemble activity in MI more accurately reconstructed a dynamically varying endpoint, whereas PMd ensemble activity more effectively predicted upcoming movements to discrete targets. Using a motor illusion paradigm, Schwartz and colleagues (2004) demonstrated that the actual arm movement trajectory was reconstructed more accurately by a population of MI neurons, whereas the visualized trajectory was reconstructed more faithfully by a population of ventral premotor cortex neurons. In the same way, the control of a robotic arm

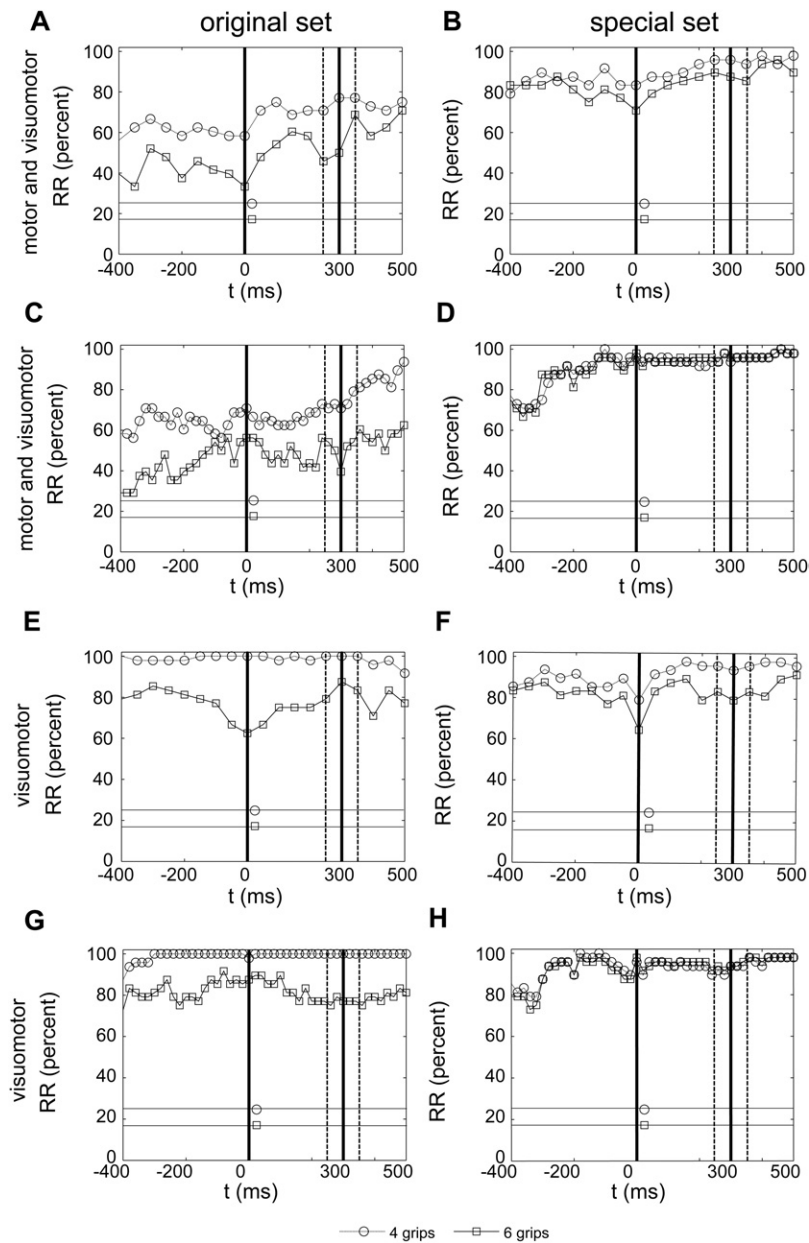


Fig. 12. Performance of the SVM classifier as a function of the number of grips to be recognized based on the features extracted during the period starting 400 ms before the instruction to move (LED color change) and ending 200 ms after the movement onset (key release) using (A, B, E, F) the sliding time window approach (sliding window width: 200 ms, moving step: 50 ms) or (C, D, G, H) the increasing time window approach (initial window width: 20 ms, increment: 20 ms). Left column: original set; right column: special set. Vertical line at 0 ms: LED color change. Vertical lines at 300 ms: mean time of key release (continuous line) \pm SD (dashed lines). Other conventions as in Fig. 5.

equipped with a dexterous hand for reaching, grasping and manipulating objects of different shape and size positioned in various spatial locations could benefit from motor, pre-motor and parietal population activity. Activity from pre-motor and parietal areas may play an instructive role for primary motor cortex during performance of skilled hand movements. For example, signals from F5 concerning the grip type, the goal of the motor act (Rizzolatti et al., 1988; Umiltà et al., 2008) and the physical properties of the object (Murata et al., 1997; Raos et al., 2006) and signals from anterior intraparietal area (AIP) providing information

about object affordances and visual guidance for the hand (Sakata et al., 1995; Murata et al., 2000; Baumann et al., 2009) could be combined with signals from MI regarding direction of reaching, timing of grasping and force to be employed. Recently, Scherberger and colleagues (Townsend et al., 2007) succeeded to correctly predict the grasp type (precision vs. power) using neural activity acquired through chronically implanted electrodes in AIP and F5. Their study is the first showing the feasibility of online grip decoding using activity recorded from pre-motor and parietal cortical areas. Our finding that the decoder cor-

rectly discriminates among grips in advance of movement onset and maintains this classification also when the movement starts, indicates that information about the grip can be provided to a control system earlier than movement onset, thus giving ample time for the control of grasping. Depending on the operation of the automatic control system, the information about the correct grip type can be used either for an early opening (during reaching) of the prosthetic hand scaled to object size, similarly to what occurs in natural reach-to-grasp movements (Jeannerod, 1981; Paulignan et al., 1990; Roy et al., 2000; Mason et al., 2001), or for a late hand opening at the end of reaching. The former solution, however, would allow a faster and smoother performance of the prosthetic hand.

Recently, Donoghue's team correlated neural activity in MI of macaques to the upper limb postures during reaching and grasping of objects differing in shape and size (Vargas-Irwin et al., 2010). They successfully measured and reconstructed 25 joint angles going far beyond the few dimensions of neural control that had been achieved so far in previous studies (Carmena et al., 2003; Hochberg et al., 2006; Kim et al., 2006; Velliste et al., 2008). However, there was no discrimination among different grips, although the task decoupled the groups of kinematic variables related to the upper arm, the wrist, and the hand. In another study Ben Hamed et al. (2007) were able to decode offline 12 single finger movements with >99% accuracy using as few as 30 neurons randomly selected from populations of task-related neurons recorded sequentially from the MI hand representation. However, movements of pairs of fingers were decoded with less accuracy (90.9%) using a three times larger population of neurons. Similar results were subsequently obtained by other studies (Acharya et al., 2008; Aggarwal et al., 2008).

The decoding performance obtained using the activity of F5 grip-related neurons is promising. The results of the present study strongly suggest that the ventral premotor area F5 is a viable cortical area that could, in combination with other areas, be proficiently used for the control of grasping.

Acknowledgments—The work described here was partly supported by the EU within the NEUROBOTICS Integrated Project (IST-FET Project 2003-001917 "The fusion of NEUROscience and roBOTICS").

REFERENCES

- Abbott LF, Dayan P (1999) The effect of correlated variability on the accuracy of a population code. *Neural Comput* 11:91–101.
- Acharya S, Tenore F, Aggarwal V, Etienne-Cummings R, Schieber MH, Thakor NV (2008) Decoding individuated finger movements using volume-constrained neuronal ensembles in the M1 hand area. *IEEE Trans Neural Syst Rehabil Eng* 16:15–23.
- Aggarwal V, Acharya S, Tenore F, Shin HC, Etienne-Cummings R, Schieber MH, Thakor NV (2008) Asynchronous decoding of dexterous finger movements using M1 neurons. *IEEE Trans Neural Syst Rehabil Eng* 16:3–14.
- Bair W, Zohary E, Newsome WT (2001) Correlated firing in macaque visual area MT: time scales and relationship to behavior. *J Neurosci* 21:1676–1697.
- Baumann MA, Fluet MC, Scherberger H (2009) Context-specific grasp movement representation in the macaque anterior intraparietal area. *J Neurosci* 29:6436–6448.
- Ben Hamed S, Schieber MH, Pouget A (2007) Decoding M1 neurons during multiple finger movements. *J Neurophysiol* 98:327–333.
- Bishop CM (1995) *Neural networks for pattern recognition*. Oxford, UK: Oxford University Press.
- Bonini L, Rozzi S, Serventi FU, Simone L, Ferrari PF, Fogassi L (2010) Ventral premotor and inferior parietal cortices make distinct contribution to action organization and intention understanding. *Cereb Cortex* 20:1372–1385.
- Borra E, Belmalih A, Gerbella M, Rozzi S, Luppino G (2010) Projections of the hand field of the macaque ventral premotor area F5 to the brainstem and spinal cord. *J Comp Neurol* 518:2570–2591.
- Brochier T, Umiltà MA (2007) Cortical control of grasp in non-human primates. *Curr Opin Neurobiol* 17:637–643.
- Burges CJC (1998) Tutorial on support vector machines for pattern recognition. *Data Min Knowl Discov* 2:121–167.
- Carmena JM, Lebedev MA, Crist RE, O'Doherty JE, Santucci DM, Dimitrov DF, Patil PG, Henriquez CS, Nicolelis MA (2003) Learning to control a brain-machine interface for reaching and grasping by primates. *PLoS Biol* 1:E42.
- Carrozza MC, Cappiello G, Micera S, Edin BB, Beccai L, Cipriani C (2006) Design of a cybernetic hand for perception and action. *Biol Cybern* 95:629–644.
- Cerri G, Shimazu H, Maier MA, Lemon RN (2003) Facilitation from ventral premotor cortex of primary motor cortex outputs to macaque hand muscles. *J Neurophysiol* 90:832–842.
- Chang CC, Lin CJ (2001) LIBSVM: a library for support vector machines. Available online: <http://www.csie.ntu.edu.tw/~cjlin/libsvm/>.
- Chen PH, Lin CJ, Scholkopf B (2005) A tutorial on v-support vector machines. *Appl Stoch Model Bus Ind* 21:111–136.
- Cortes C, Vapnik V (1995) Support-vector networks. *Mach Learn* 20:273–297.
- Duin RPW, Juszczak P, Palick P, Pekalska E, de Ridder D, Tax DMJ (2004) PRTools4. A Matlab toolbox for pattern recognition. Available online: <http://www.prtools.org/files/PRTools4.1.pdf>.
- Dum RP, Strick PL (1991) The origin of corticospinal projections from the premotor areas in the frontal lobe. *J Neurosci* 11:667–689.
- Dum RP, Strick PL (2005) Frontal lobe inputs to the digit representations of the motor areas on the lateral surface of the hemisphere. *J Neurosci* 25:1375–1386.
- Fattori P, Raos V, Breviglieri R, Bosco A, Marzocchi N, Galletti C (2010) The dorsomedial pathway is not just for reaching: grasping neurons in the medial parieto-occipital cortex of the macaque monkey. *J Neurosci* 30:342–349.
- Fukunaga K (1990) *Introduction to statistical pattern recognition*. San Diego, CA, USA: Academic Press.
- Gardner EP, Babu KS, Ghosh S, Sherwood A, Chen J (2007a) Neurophysiology of prehension. III. Representation of object features in posterior parietal cortex of the macaque monkey. *J Neurophysiol* 98:3708–3730.
- Gardner EP, Babu KS, Reitzen SD, Ghosh S, Brown AS, Chen J, Hall AL, Herzlinger MD, Kohlenstein JB, Ro JY (2007b) Neurophysiology of prehension. I. Posterior parietal cortex and object-oriented hand behaviors. *J Neurophysiol* 97:387–406.
- Hatsopoulos N, Joshi J, O'Leary JG (2004) Decoding continuous and discrete motor behaviors using motor and premotor cortical ensembles. *J Neurophysiol* 92:1165–1174.
- Hatsopoulos NG, Donoghue JP (2009) The science of neural interface systems. *Annu Rev Neurosci* 32:249–266.
- He SQ, Dum RP, Strick PL (1993) Topographic organization of corticospinal projections from the frontal lobe: motor areas on the lateral surface of the hemisphere. *J Neurosci* 13:952–980.
- Hochberg LR, Serruya MD, Friehs GM, Mukand JA, Saleh M, Caplan AH, Branner A, Chen D, Penn RD, Donoghue JP (2006) Neuronal ensemble control of prosthetic devices by a human with tetraplegia. *Nature* 442:164–171.

- Hsu CW, Chang CC, Lin CJ (2003) A practical guide to support vector classification. Available online: www.csie.ntu.edu.tw/~cjlin/papers/guide/guide.pdf.
- Huang TK, Weng PC, Lin CJ (2006) Generalized Bradley-Terry models and multi-class probability estimates. *J Mach Learn Res* 7:85–115.
- Jeannerod M (1981) Intersegmental coordination during reaching at natural visual objects. In: Attention and performance (Long J, Baddeley A, eds), pp 153–168. Hillsdale, NJ: Erlbaum.
- Kapandji IA (1982) Upper limb. In: The physiology of the joints, Vol. 1. New York: Churchill Livingstone.
- Keerthi SS (2002) Efficient tuning of SVM hyperparameters using radius/margin bound and iterative algorithms. *IEEE Trans Neural Netw* 13:1225–1229.
- Kim HK, Biggs SJ, Schloerb DW, Carmena JM, Lebedev MA, Nicolelis MA, Srinivasan MA (2006) Continuous shared control for stabilizing reaching and grasping with brain-machine interfaces. *IEEE Trans Biomed Eng* 53:1164–1173.
- Lebedev MA, O'Doherty JE, Nicolelis MA (2008) Decoding of temporal intervals from cortical ensemble activity. *J Neurophysiol* 99:166–186.
- Light CM, Chappell PH (2000) Development of a lightweight and adaptable multiple-axis hand prosthesis. *Med Eng Phys* 22:679–684.
- Mason CR, Gomez JE, Ebner TJ (2001) Hand synergies during reach-to-grasp. *J Neurophysiol* 86:2896–2910.
- Matelli M, Camarda R, Glickstein M, Rizzolatti G (1986) Afferent and efferent projections of the inferior area 6 in the macaque monkey. *J Comp Neurol* 251:281–298.
- Matelli M, Luppino G, Rizzolatti G (1985) Patterns of cytochrome oxidase activity in the frontal agranular cortex of the macaque monkey. *Behav Brain Res* 18:125–136.
- Matsumura M, Kubota K (1979) Cortical projection to hand-arm motor area from post-arcuate area in macaque monkeys: a histological study of retrograde transport of horseradish peroxidase. *Neurosci Lett* 11:241–246.
- Maynard EM, Hatsopoulos NG, Ojakangas CL, Acuna BD, Sanes JN, Normann RA, Donoghue JP (1999) Neuronal interactions improve cortical population coding of movement direction. *J Neurosci* 19:8083–8093.
- Muakkassa KF, Strick PL (1979) Frontal lobe inputs to primate motor cortex: evidence for four somatotopically organized “premotor” areas. *Brain Res* 177:176–182.
- Murata A, Fadiga L, Fogassi L, Gallese V, Raos V, Rizzolatti G (1997) Object representation in the ventral premotor cortex (area F5) of the monkey. *J Neurophysiol* 78:2226–2230.
- Murata A, Gallese V, Kaseda M, Sakata H (1996) Parietal neurons related to memory-guided hand manipulation. *J Neurophysiol* 75:2180–2186.
- Murata A, Gallese V, Luppino G, Kaseda M, Sakata H (2000) Selectivity for the shape, size, and orientation of objects for grasping in neurons of monkey parietal area AIP. *J Neurophysiol* 83:2580–2601.
- Musallam S, Corneil BD, Greger B, Scherberger H, Andersen RA (2004) Cognitive control signals for neural prosthetics. *Science* 305:258–262.
- Nicolelis MA, Lebedev MA (2009) Principles of neural ensemble physiology underlying the operation of brain-machine interfaces. *Nat Rev Neurosci* 10:530–540.
- Paulignan Y, MacKenzie C, Marteniuk R, Jeannerod M (1990) The coupling of arm and finger movements during prehension. *Exp Brain Res* 79:431–435.
- Raos V, Franchi G, Gallese V, Fogassi L (2003) Somatotopic organization of the lateral part of area F2 (dorsal premotor cortex) of the macaque monkey. *J Neurophysiol* 89:1503–1518.
- Raos V, Umiltà MA, Gallese V, Fogassi L (2004) Functional properties of grasping-related neurons in the dorsal premotor area F2 of the macaque monkey. *J Neurophysiol* 92:1990–2002.
- Raos V, Umiltà MA, Murata A, Fogassi L, Gallese V (2006) Functional properties of grasping-related neurons in the ventral premotor area F5 of the macaque monkey. *J Neurophysiol* 95:709–729.
- Rizzolatti G, Camarda R, Fogassi L, Gentilucci M, Luppino G, Matelli M (1988) Functional organization of inferior area 6 in the macaque monkey. II. Area F5 and the control of distal movements. *Exp Brain Res* 71:491–507.
- Roy AC, Paulignan Y, Farne A, Joffrais C, Boussaoud D (2000) Hand kinematics during reaching and grasping in the macaque monkey. *Behav Brain Res* 117:75–82.
- Rozzi S, Ferrari PF, Bonini L, Rizzolatti G, Fogassi L (2008) Functional organization of inferior parietal lobule convexity in the macaque monkey: electrophysiological characterization of motor, sensory and mirror responses and their correlation with cytoarchitectonic areas. *Eur J Neurosci* 28:1569–1588.
- Sakata H, Taira M, Murata A, Mine S (1995) Neural mechanisms of visual guidance of hand action in the parietal cortex of the monkey. *Cereb Cortex* 5:429–438.
- Santello M, Flanders M, Soechting JF (1998) Postural hand synergies for tool use. *J Neurosci* 18:10105–10115.
- Santhanam G, Ryu SI, Yu BM, Afshar A, Shenoy KV (2006) A high-performance brain-computer interface. *Nature* 442:195–198.
- Schieber MH, Santello M (2004) Hand function: peripheral and central constraints on performance. *J Appl Physiol* 96:2293–2300.
- Schmidlin E, Brochier T, Maier MA, Kirkwood PA, Lemon RN (2008) Pronounced reduction of digit motor responses evoked from macaque ventral premotor cortex after reversible inactivation of the primary motor cortex hand area. *J Neurosci* 28:5772–5783.
- Schwartz AB, Cui XT, Weber DJ, Moran DW (2006) Brain-controlled interfaces: movement restoration with neural prosthetics. *Neuron* 52:205–220.
- Schwartz AB, Moran DW, Reina GA (2004) Differential representation of perception and action in the frontal cortex. *Science* 303:380–383.
- Serruya MD, Hatsopoulos NG, Paninski L, Fellows MR, Donoghue JP (2002) Instant neural control of a movement signal. *Nature* 416:141–142.
- Shawe-Taylor J, Cristianini N (2004) Kernel methods for pattern analysis. Cambridge, UK: Cambridge University Press.
- Shimazu H, Maier MA, Cerri G, Kirkwood PA, Lemon RN (2004) Macaque ventral premotor cortex exerts powerful facilitation of motor cortex outputs to upper limb motoneurons. *J Neurosci* 24:1200–1211.
- Sigurdsson S (2002) The ANN:DTU toolbox. Available online: <http://isp.imm.dtu.dk/toolbox/menu.html>.
- Soechting JF, Flanders M (1997) Flexibility and repeatability of finger movements during typing: analysis of multiple degrees of freedom. *J Comput Neurosci* 4:29–46.
- Taylor DM, Tillery SI, Schwartz AB (2002) Direct cortical control of 3D neuroprosthetic devices. *Science* 296:1829–1832.
- Townsend BR, Lehmann SJ, Subasi E, Scherberger H (2007) Decoding hand grasping signals from primate premotor and parietal cortex. Program No 41416, 2007 Neuroscience Meeting Planner, San Diego, CA: Society for Neuroscience, 2007 Online.
- Umiltà MA, Brochier T, Spinks RL, Lemon RN (2007) Simultaneous recording of macaque premotor and primary motor cortex neuronal populations reveals different functional contributions to visuomotor grasp. *J Neurophysiol* 98:488–501.
- Umiltà MA, Escola L, Intskirveli I, Grammont F, Rochat M, Caruana F, Jezzini A, Gallese V, Rizzolatti G (2008) When pliers become fingers in the monkey motor system. *Proc Natl Acad Sci U S A* 105:2209–2213.
- Vargas-Irwin CE, Shakhnarovich G, Yadollahpour P, Mislow JM, Black MJ, Donoghue JP (2010) Decoding complete reach and grasp actions from local primary motor cortex populations. *J Neurosci* 30:9659–9669.

Velliste M, Perel S, Spalding MC, Whitford AS, Schwartz AB (2008) Cortical control of a prosthetic arm for self-feeding. *Nature* 453:1098–1101.

Wessberg J, Stambaugh CR, Kralik JD, Beck PD, Laubach M, Chapin JK, Kim J, Biggs SJ, Srinivasan MA, Nicolelis MA (2000) Real-time

prediction of hand trajectory by ensembles of cortical neurons in primates. *Nature* 408:361–365.

Zohary E, Shadlen MN, Newsome WT (1994) Correlated neuronal discharge rate and its implications for psychophysical performance. *Nature* 370:140–143.

(Accepted 29 April 2011)